Iraqi Journal of Industrial Research (IJOIR)

Journal homepage: http://ijoir.gov.iq

Enhancement of Mechanical Behaviour of Functionally Graded Viscoelastic Materials Parts Reinforced by Hybrids Nanoparticles

Emad Kadum Njim*, Fadhel Abbas Hadi, Naeem Abdulmohsin Alhilo

State Company for Rubber and Tires Industries, Ministry of Industry and Minerals – Iraq

Article information

Article history:
Received: December, 15, 2022
Accepted: May, 10, 2023
Available online: October, 20, 2023

Keywords:
FGVE,
Static analysis,
Hybrid nanomaterials,
FEM

Corresponding Author:
Emad Kadum Njim
emad.njim@gmail.com

DOI:
https://doi.org/10.53523/ijoirVol10I2ID287

Abstract

This paper studies the mechanical behavior of functionally graded material viscoelastic (FGVE) products employed in automotive, chemical industry, and biomedical appliances. Various experimental models describe and simulate nanobeams with viscoelastic layers subjected to tensile loading, 3-point bending, tear, and impact. All specimens were prepared using the 3D printing method. Tensile, hardness, tear, impact, and bending specimens reinforced with different volume fractions (1-5)% of Al_2O_3, TiO_2, and a hybrid of the nanomaterials Al_2O_3 /TiO_2 were arranged via a mixing process with an extruder and then fabricated by a 3D printing machine. The experimental results of maximum bending load, midspan deflection, impact, and tear resistance were validated by finite element methods (FEM) with the assistance of commercial software (Ansys Workbench 2021 R1). Furthermore, the influence of various parameters on the mechanical performance of reinforced samples has been thoroughly investigated, for example, volume fraction index, nanoparticles content, and FG properties. Based on the findings, the most successful results were obtained by adding 1.5 % Al_2O_3 and 3% TiO_2 hybrid nanoparticles. The experimental and numerical results were in reasonable agreement. The discrepancy did not exceed 10.25% for maximum bending load and no difference over 5% for maximum impact load, indicating that the strengthened nanoparticle specimens were properly fabricated. Also, a significant improvement in mechanical and viscoelastic properties was achieved by incorporating hybrid nanoparticles. Flexural bending load increased by about 17 % with hybrid nanoparticles, while tear resistance increased by 27.5 % and impact resistance increased by 7.5%.

1. Introduction

Nano Developing advanced engineering designs is necessary to meet the demands of engineering applications. These designs are made more efficient using advanced composite materials that hold up to various challenges. This light structure has a high stiffness or strength-to-weight ratio. Viscoelastic materials are now used for various applications, such as biomaterials, aerospace, energy, automobiles, and sports facilities. Creep interaction, fatigue cracks, and significant dynamic response are some of the characteristics of these materials.

Because of their viscoelastic nature, viscoelastic materials absorb and dampen vibrational energy. Besides being efficient shock absorbers, viscoelastic materials also have excellent elasticity. Rubber-like compounds are elastomers; they are extremely viscoelastic and excellent impact absorbers.

The viscoelastic behavior of polymeric materials can be investigated and characterized experimentally. One such method consists of stress relaxation measurements. Under this approach, the polymer sample is firstly strained rapidly in tension to some fixed strain value while its temperature is kept constant. The experiment then measures the stress required for maintaining this strain level across the polymer sample at its fixed and predefined value, which typically decreases with time owing to the time-dependent nature of viscoelasticity and its associated molecular relaxation processes. The ratio between this measured time-dependent stress profile and the fixed predefined value of the strain is called the relaxation modulus of the viscoelastic polymer [1].

Furthermore, viscoelastic materials and polymers are often employed as dampeners in constructing skyscrapers when such tall buildings are subject to significant vibrations caused by wind or earthquakes. When acting as dampeners, viscoelastic materials can absorb such vibrational energy. Another application of viscoelastic polymers as vibrational dampeners is in the insulation of helicopter fuselages from the noise made by the main rotor. Polylactic acid (PLA) is a thermoplastic having outstanding mechanical performance, thermal stability, flexibility, and suitable fabricating ability. “PLA” melt, like other plastic polymers, is viscoelastic. It has a flow pattern that combines permanent flow behavior caused by polymer microstructure breakdown with controllable deformations caused by biochemical interconnectedness [2]. Extensive research has been conducted on the static and dynamic response of plates, shells, and beams comprised of (honeycomb, foam, FGM), and viscoelastic materials [3-6]. Developing VE aims to reduce imperfections caused by manufacturing processes in composite constructions. In contrast, VE materials have been used in sandwich constructions, such as laminated composite or FGM structures, due to the progressive modification of material characteristics at the interfaces between the face layers. Because these structures are typically employed in thermal applications [7], assessing their static and dynamic characteristics is essential.

Ariza Gomez et al. [8] investigated and introduced the bending issue of VE structures with certain essential characteristics such as volume fraction index, support and loading circumstances, and beam arrangement. Yun Gao et al. [9] investigated the bending creep behavior of viscoelastic laminated arches with interlayers under a distributed load. Shengwei Chen et al. [10] investigated the impact of a biomaterial composite consisting of a stiff 3D printed frame and a soft viscoelastic foam used for protection applications by employing experimental work. Xavior et al. [11] conducted a more in-depth experimental study of the failure of split FG beams made of porous polymer materials utilizing flexural, tensile, and compressive experimental procedures. Ali Dogan [12] used an analytical model to investigate the quasi-static and dynamic behavior of FGM viscoelastic plates under dynamic loads. The acquired findings were compared to the FEM approach results. Nishant Kumar et al. [13] used the shear deformation theory to conduct free vibration research on doubly curved sandwich shell panels with a viscoelastic core limited by a functionally graded material layer. Many nanostructures with varied capabilities and purposes may be built in nanotechnology, and the nanosurface effect can significantly impact a nanostructure's performance. FGM nanostructures have been successfully used for static and dynamic analysis due to their constant change of properties from one surface to the next [14-16]. The bending behavior of TiO2 nanoparticle-reinforced carbon/epoxy composites was examined by Yadhav et al. [17]. Pengfei et al., in their work, investigated the static and dynamic properties of FG piezoelectric nanobeams with dynamic flexoelectricity [18].

Furthermore, composite and FG nanostructures' dynamic and thermal behavior has been studied using the finite element method and experimental works [19, 20]. Koutoati et al. [21] investigated the static and vibration assessments of FGM viscoelastic sandwich beams with the nonlinear material feature using a finite element approach. Alavi et al. [22] employed analytical modeling based on first-order deformation theory and ABAQUS software to investigate the dynamic behavior of viscoelastic FG porous plates under various hybrid loadings. Hai et al. [23] investigated forced analysis on cross/angle-ply laminated composite nanoplates resting on viscoelastic foundations using higher-order shear deformation theory. Ruifang Shi et al. [24] investigated the mechanical and viscoelastic characteristics of rubber nanocomposites loaded with silica nanoparticles. The inclusion of silica nanoparticles results in considerable changes in static distribution, mobility, and bond orientation. Recently M. Al-Shablle et al. [25] analyzed the dynamic response of rubber composite nanobeams using two nanoparticles, Al_2O_3 and SiO_2.

According to the literature, few studies on the static and dynamic analysis of functionally graded viscoelastic nanobeams have been undertaken, and a few researchers included just numerical and analytical data without addressing practical work with FGVE beams. The present investigation aims to examine the influence of nanomaterial reinforcement on the mechanical properties of FGVE materials. A mathematical model is developed to calculate the beam's general mechanical properties, the maximum bending strength load, the deflections, and the impact. Various experiments on 3D printed samples are carried out based on various parameters (volume fraction index, geometrical properties, viscoelastic material type, and nanoparticles types). The experimental results were validated using the finite element technique (FEM). The following describes how this paper is organized: The second section provides a theoretical foundation for the functionally graded viscoelastic material structure. Section 3 describes a numerical approach for checking results. Section 4 gives the results of the different mechanical testing of the viscoelastic samples, along with useful commentary. Section 5 of this research offers several critical notes relating to the performance of nano-reinforced viscoelastic materials and helpful suggestions for further development.

2. Theoretical Part

This optional Consider a functionally graded material viscoelastic (FGVE) beam that is made of one constituent, such as rubber or polylactic acid (PLA), which are commonly found in biological tissues. As illustrated in Figure (1), the suggested representation for the material constituents according to the porosity distribution (α) might be considered to be in the form [26] of a beam dimension (length L and thickness h) and by adopting a power-law distribution scheme (n).

$$\boldsymbol{V_p(z) = V_m - \alpha . V_m \left(\frac{z}{h} + \frac{1}{2}\right)^n} \qquad (1)$$

where n indicates a volume variation exponent in which n ε [0, ∞) that explains the change in thickness of material properties. Generally, the porous beam is considered a VE beam. In the current investigation, the novel FGVE beam is considered to be made up of only one component. Polymer core with an identical porosity volume fraction arrangement (α) and graded through-beam thickness. Hence, For example, n = 0, V_p (z) = V_m – αV_m while n =∞, (V_p=V_m=1), where (V_p) is the entire volume of polymer with porosity, and (V_m) is the volume of base metal Consequently, the proposed mechanical properties of the FGVE beam can be represented as [27]

$$\boldsymbol{Q(z) = Q_m - \alpha . Q_m \left(\frac{z}{h} + \frac{1}{2}\right)^n} \qquad (2)$$

Q_m denotes the metal material qualities of the VE functionally graded beam. Hence, the perfect beam (porosity = 0), whereas for the porous VE beam, the metal property characteristics of the FGVE beam: Young's modulus (E), and mass density (ρ) may be represented as,

$$\boldsymbol{E(z) = E_m - E_m \alpha \left(\frac{z}{h} + \frac{1}{2}\right)^n} \qquad (3)$$

$$\boldsymbol{\rho(z) = \rho_m - \rho_m \alpha \left(\frac{z}{h} + \frac{1}{2}\right)^n} \qquad (4)$$

The total deflection ($\boldsymbol{\delta_T}$) owing to bending and shear near the midspan of the beam in a 3-point bending test may be calculated using the following equation [28],

$$\boldsymbol{\delta_T = \delta_b + \delta_s = \frac{Fl^3}{48(EI)_{eq.}} + \frac{Fl}{4(AG)_{eq.}}} \qquad (5)$$

Here, F is the applied force, l is the span of the beam, I is the total moment of inertia; (A) is the beam's cross-sectional area, and G is its length (the modulus of shear). As a result, the total rigidity of both of these parts will be

$$\boldsymbol{E_{eq.} = E(z) = E_m - E_m \alpha \left(\frac{z}{h} + \frac{1}{2}\right)^n} \qquad (6)$$

Moreover, the equivalent shear rigidity ($AG_{eq.}$) becomes,

$$(AG)_{eq.} = bhG_{eq.} \qquad (7)$$

The symbols h and b denote the thickness and width of the beam, accordingly. For a rectangular cross-section, the bending stress f may be computed as follows:

$$\sigma_f = \frac{3FL}{2bh^2} \qquad (8)$$

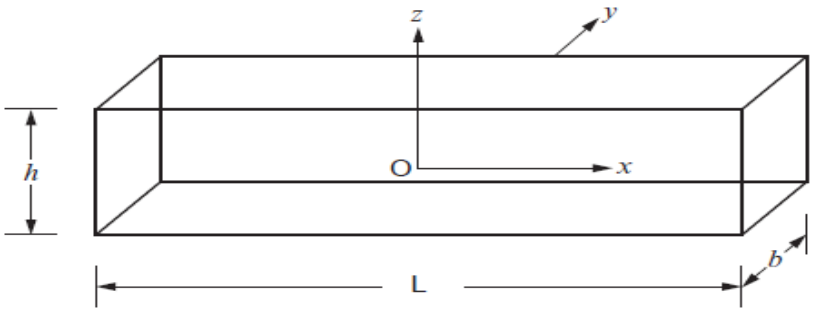

Figure (1). The geometry of the beam.

3. Experimental Procedure

a. Material and Methods

PLA materials, which are extensively used in engineering fields, are used in this work. The materials were purchased internationally to conduct tensile, impact, and bending tests. For each test, two samples were created: one with a uniform density and the other with varying densities and thicknesses. Hybrid nanomaterials consisting of Aluminum Oxide Nanoparticles (Al_2O_3) and Titanium Oxide (TiO_2) with various volume fractions were fabricated for both perfect and FGVE porous polymers.

b. Sample Preparation

Heating methods like injection molding and extrusion convert PLA polymers into geometric shapes. The following schematic shows fabricating viscoelastic materials samples reinforced with hybrid nanomaterials (Al_2O_3 and TiO_2). Specimens for each test were manufactured per industry standards. First, 1.75 mm polymer wire was injected into the simply supported (SS) cylinder of the polymer lab small laboratory screw extrusion process as raw material. The Al_2O_3 nanoparticles are then properly weighed before being fed into the extruder and mixed with polymer wire. When time and temperature are satisfied, polymer flow through the extruder head produces a filament nano polymer with the appropriate dimensions and characteristics. A micrometer is used to measure the diameter precisely (0.001). Finally, a new wire is used with CR-10 MAX 3D printing tools. The investigated examples were generated using a suitable computer program, with the geometry saved as a (.stl) file and the final shape printed on a 3D printer. Figure (2) depicts the nano FGVE beam processing technique.

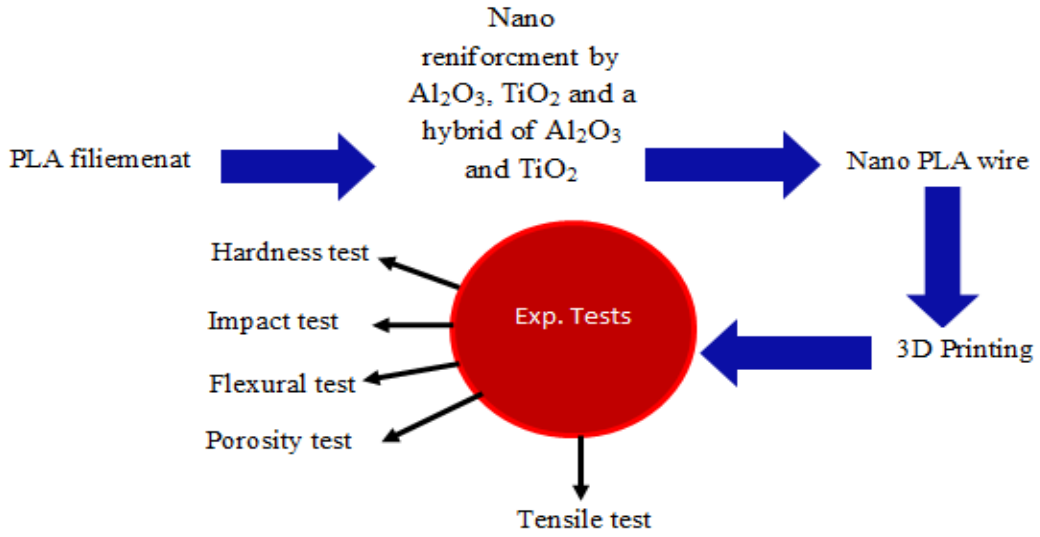

Figure (3). The flow chart of experimental work.

The Tensile Strength Test

Tensile characteristics are utilized to choose between various materials. Tensile properties are regularly tested to verify if they fulfill the requirements stated in their specifications. The picture geometry and specimen dimensions are depicted in Figure (4 a). Polymer samples shown in Figure (4 b) were created using 3D printing following ASTM standard D638 [29]. A digital universal testing apparatus is shown in Figure (5), performing uniaxial tensile tests with the cross-head speed was 1 mm/min during all experiments. The polymer samples' tensile strength has been restricted. The findings of stress-strain measurements on 3D-printed materials subjected to tensile loading are shown in Figure (6). As an additional measure of accuracy, the results contain an average of six measurements for the polymer specimens.

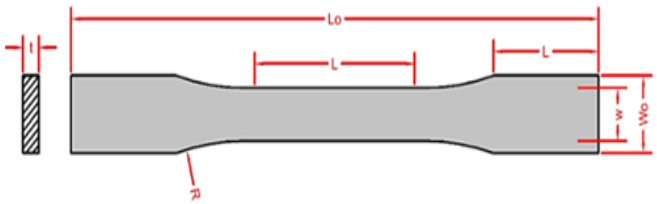

L_o= 165 mm, L= 33 mm, W_o =20 mm, W= 12.5mm, t=3mm, R= 76 mm, Gauge length= 50 mm.

-a-

-b-

Figure (4). (a) Tensile sample (mm) construction following ASTM standard D3763, (b) 3D printed polymer tensile samples**.**

Figure (5). Tensile Strength test machine.

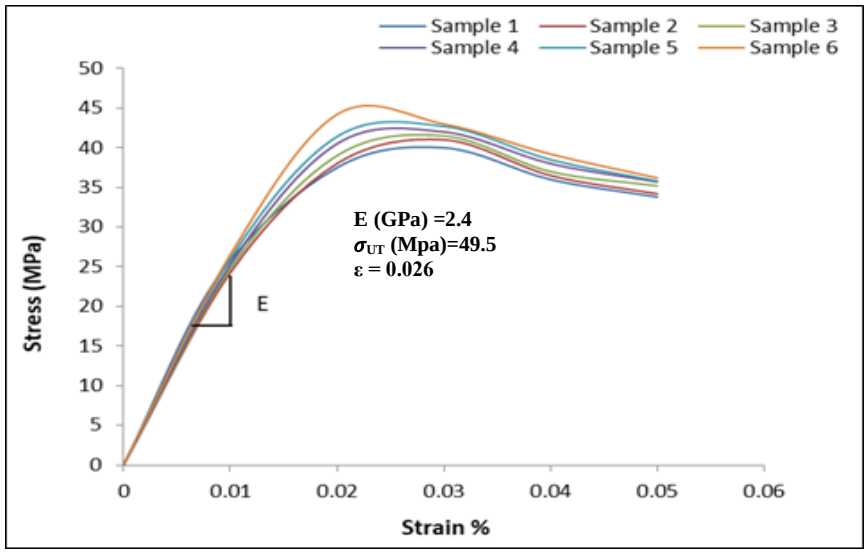

Figure (6). PLA samples stress-strain curves under tensile load.

Flexural Test

This study aims to develop a porosity arrangement model for FG viscoelastic materials. The volume fraction of the pore region in this design frequently exhibits a power-law distribution. 3D printing is a rising processing technique that uses CAD software to create three-dimensional samples or scan the designed items. During this procedure, metallic wires are melted within the head of printers. The filament is introduced to the nozzle, causing the fabricated wire to be discharged. Successive layers of material are melted during treatment to produce designed models. A z-axis moving bench supports the workpiece.

Consequently, It will create a 3D form equivalent to the one specified. PLA, a primary source and ideal for most industrial, medical, and home uses, are one of the most regularly used materials for 3D printing [2]. The polymer specimens were fabricated in local markets following ASTM standard D790 [30], with dimensions L=60 mm, W=10 mm, with porosity parameters (10%, 20%, 30%) and power law index 0.5, 1, and 2. Sandwich panels are often tested for their bending performance and impact resistance using the 3-point bending test.

A beam's flexural strength, stiffness, and beam shear modulus are calculated based on the flexural strength of the materials and structures. A test specimen of rectangular cross section rests on two supports (10 mm in diameter) in a flat-wise position and is loaded with a loading nose located midway between the supports. A transducer, deflectometer, or dial gauge can measure midspan deflection. The crosshead speed is maintained at 4 mm/second with a simply supported rig. A transducer, deflectometer, or dial gauge can measure midspan deflection. Load-deflection curves can be generated using load-deflection curves applied to the specimen's center to determine sandwich stiffness and shear modulus. A total of fifteen (15) FG samples were measured using three-point bending for each porosity parameter value. FGVE beam experimental setup is shown in Figure (7).

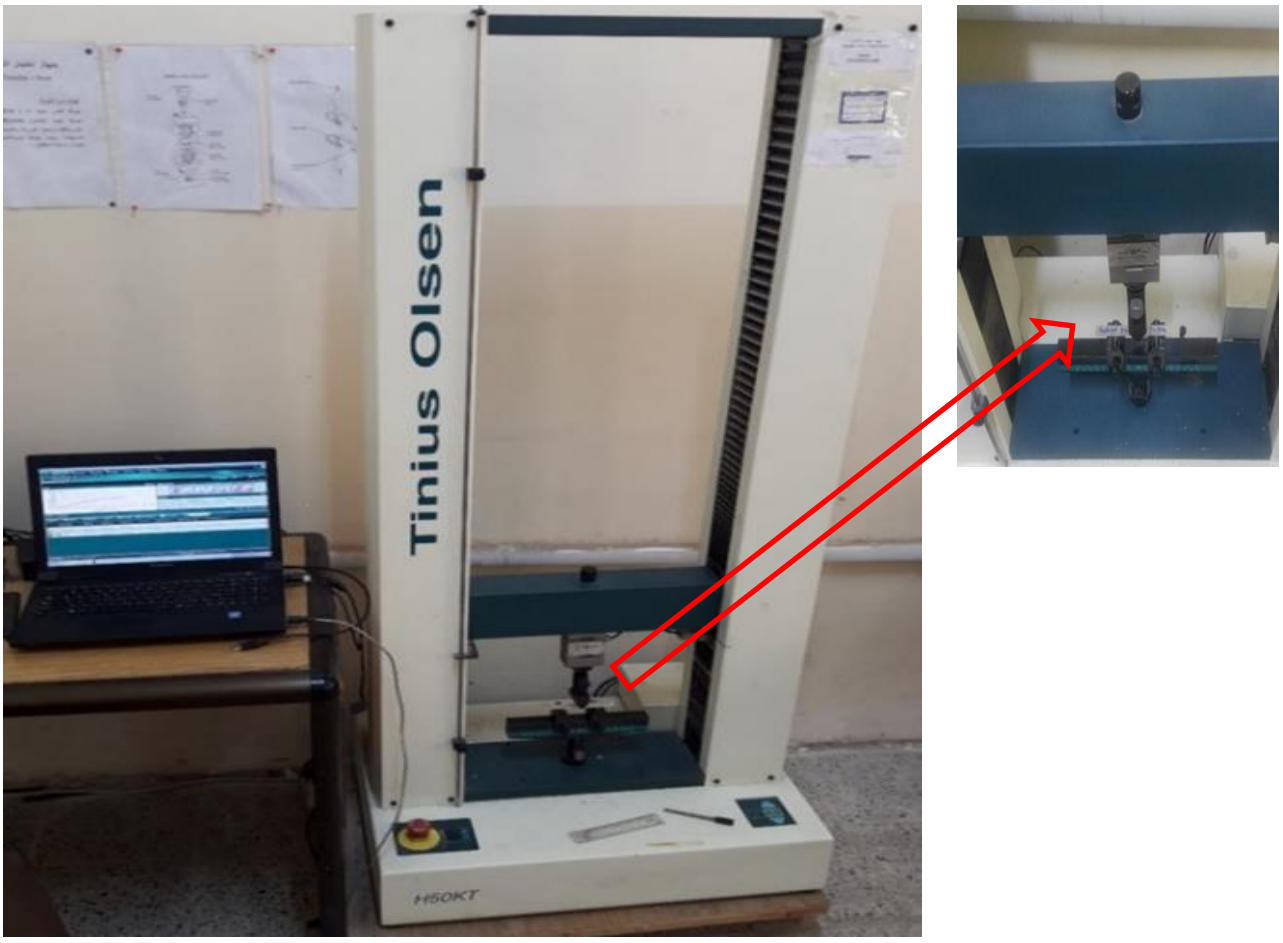

Figure (7). Experimental setup for the FG beam.

Impact Test

The impact tests were conducted using the impact apparatus (Type GUNT Hamburg), as shown in Figure (8). Impact test was done using un-notched Charpy-Impact testing equipment with ASTM D256 standard with a specimen having a rectangle shape of 55 × 10 × 6 mm.

For the impact test, the computation of impact strength and fracture toughness relies upon the needed energy computation for the fracture [31]. The impact strength can be found as follows:

$$Gc = Uc / A \qquad (9)$$

Where (G_c) is the material's impact strength (J/m^2), (U_c) is the absorbed energy (J), and (A) is the specimen's cross-sectional area (m^2). Figure (8) illustrates the experimental apparatus of the impact test.

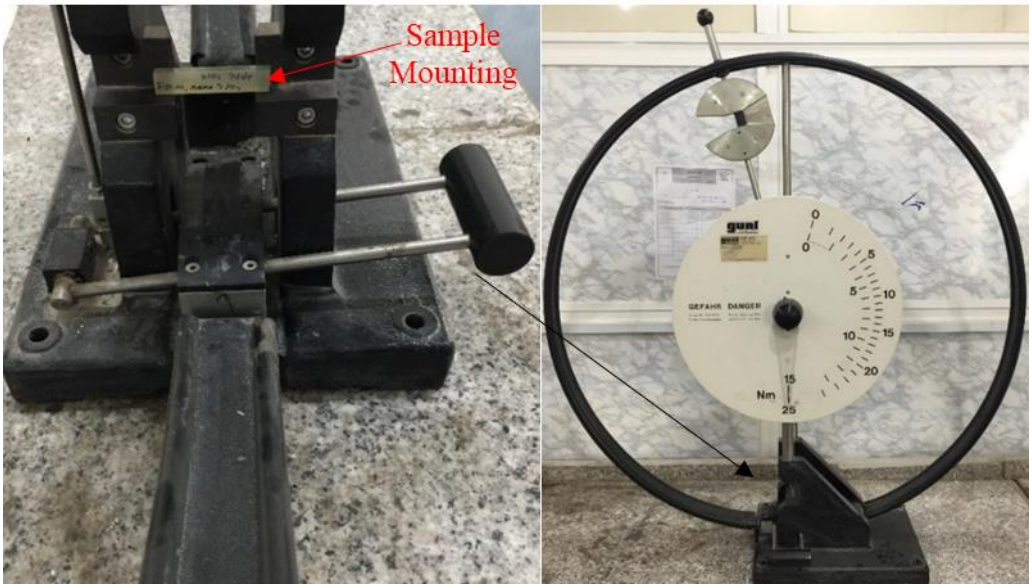

Figure (8). Experimental setup for impact test.

4. Finite Element Analysis

The reliability of numerical findings is evaluated using a finite element model (FEM) and three-point bending measurements [32-34]. ANSYS 2021 R1 was used to investigate the flexural behavior of the FGVE beam. As demonstrated in Figure (9), the model is built using the SHELL99 composite element type, with 20149 total elements and 25988 nodes. Following convergence mesh research, model boundary constraints were used. The load is delivered progressively, as indicated in Figure (10), and supported boundary conditions are utilized.

The effective material characteristics are determined using a power-law model of the mixing rule (Equations 2-4) and then entered into ANSYS' engineering library view.

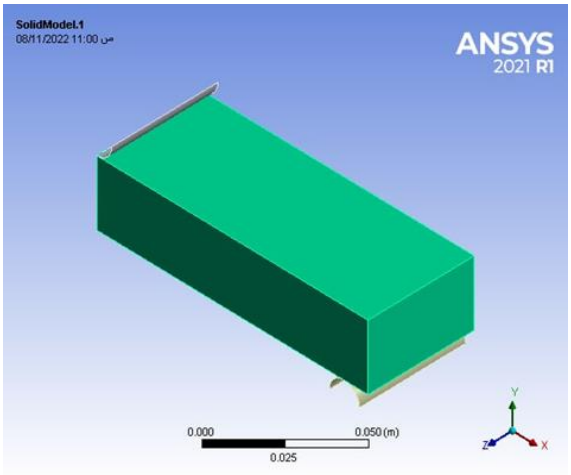

Figure (9). A generated three-dimension model of the FGVE beam.

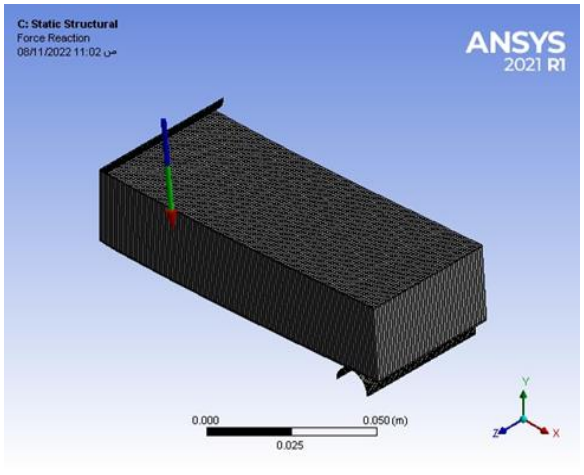

Figure (10). The built geometry with boundary conditions.

5. Results and Discussion

The influence of nanoparticles V_f and FG parameters on the performance of FGVE samples is examined in this part. A Universal Testing Machine (UTM) was employed to test samples for tensile and 3-point bending, while the GUNT instrument was used to conduct impact tests, considering three different types of nanoparticle

constituents: Al_2O_3, TiO_2, and hybrid Al_2O_3/TiO_2 and with FG gradient index (n = 0.5, 1, and 2). The experimental findings, such as the maximum bending load and total deflection at midspan, were obtained using a PC connected to the testing apparatus.

Figure (11 – 14) depicts the force-displacement curves for simply supported FGVE beams without nanoparticles and with Al_2O_3, TiO_2, and hybrid nanoparticles, an FG exponent of (n=1), and a sample height of 6 mm. According to the results, the hybrid nanoparticle (1.5 % V_f Al_2O_3 and 3% V_f TiO_2) reinforced FGVE beams exhibit improved bending strength with a significant increase of (10%). Based on ANSYS 2021 R1, the results of three-point bending are validated, as shown in Figures (15–18). According to the data, the flexural force increases as the gradient index value increases. There might be a 10% variation between experimental and numerical bending load results. Additionally, hybrid nanoparticle samples bend more than Al_2O_3 or TiO_2 nanoparticle samples.

Tables (1 & 2) present experimental and numerical results of maximum bending load at four values of V_f (0.5,1 2, and 5) using Al_2O_3 and TiO_2 nano samples, respectively, while Table (3) shows similar results using four percentages of V_f (1.5/1, 1.5/1.5, 1.5/3, and 1.5/5) hybrid nanoparticles. It is observed from the obtained numerical results that the maximum bending load increases with increasing power-law index; this may be because strength improves significantly.

The bending stress variation between experimental and numerical models is less than 10% in all cases. This percentage depends on the power-law index and the V_f % of the same FGVE beam geometrical properties. Figure 19 shows the experimental maximum deflection load (mm) for FGVE beams reinforced with three different types of nanoparticles. Accordingly, we can conclude that the maximum deflection decreases as the gradient index factor increases. A similar effect was achieved by using nanoparticles to strengthen the beam's resistance to deformation. The most significant observation based on the configuration of defective specimens observed throughout the experiments is that beam yielding is the most common cause of beam failure, and shear may be the cause of beam deformation, which occurs in PLA layers with a high V_f percentage and nanoparticle concentration and can cause beam failure. Table (4) shows the calculated and experimental maximum bending deflection at the beam midspan for n=1 and four V_f values (0.5, 1, 1.5, and 5) with Alumina and TiO_2 types of nanoparticles, respectively. Besides various mixing ratios (1.5/1, 1.5/1.5, 1.5/3, and 1.5/5) hybrid nanoparticles. It is noticed that samples with hybrid nanoparticles exhibit less deflection than other types.

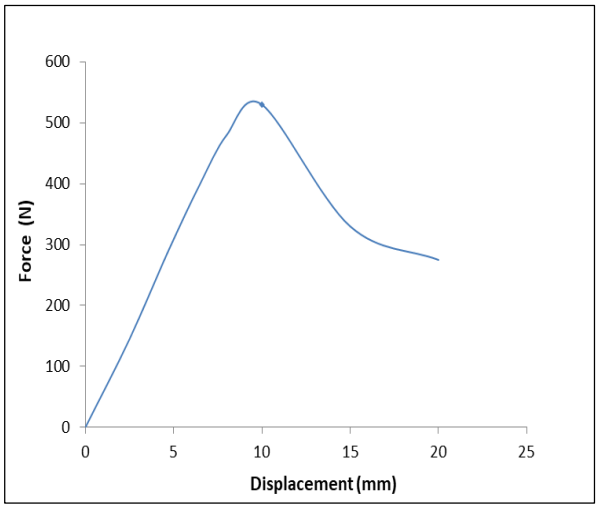

Figure (11). The experimental force-displacement curve without nanoparticles (n = 1).

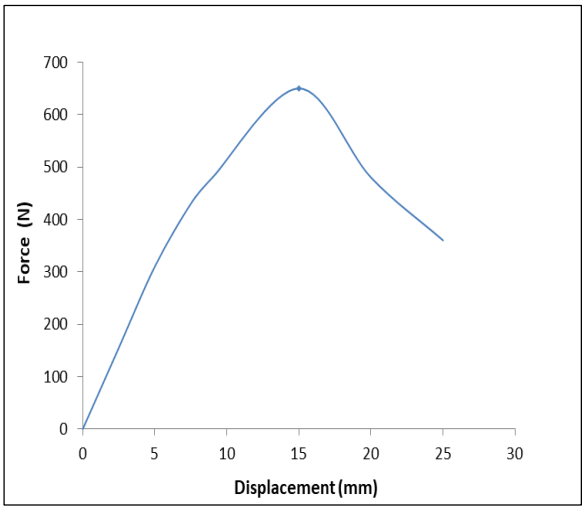

Figure (12). The experimental force-displacement curve with 1.5 % Al_2O_3 nanoparticles (n = 1).

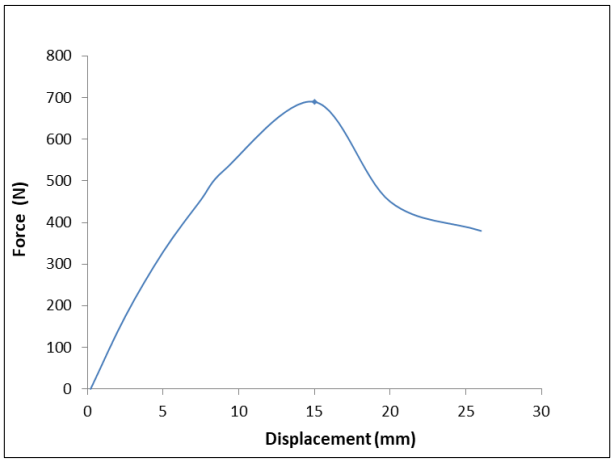

Figure (13). The experimental force-displacement curve with 1.5 % TiO_2 nanoparticles (n = 1).

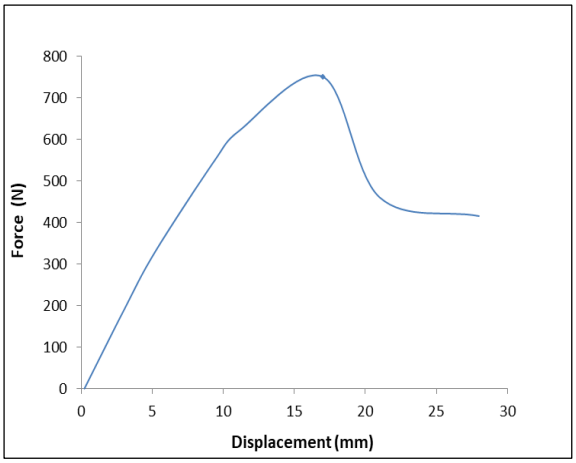

Figure (14). The experimental force-displacement curve with hybrid nanoparticles (1.5 % Al_2O_3- 3% TiO_2 at n = 1).

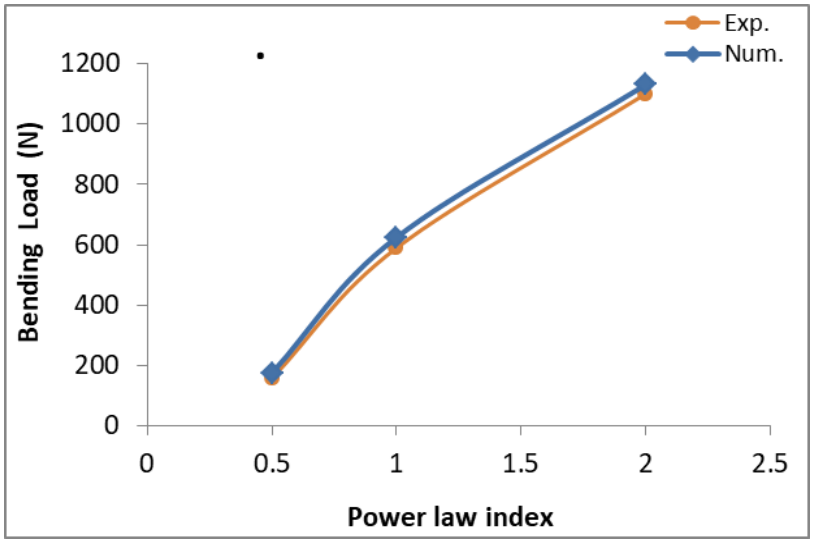

Figure (15). The results of bending load (N) without nanoparticles.

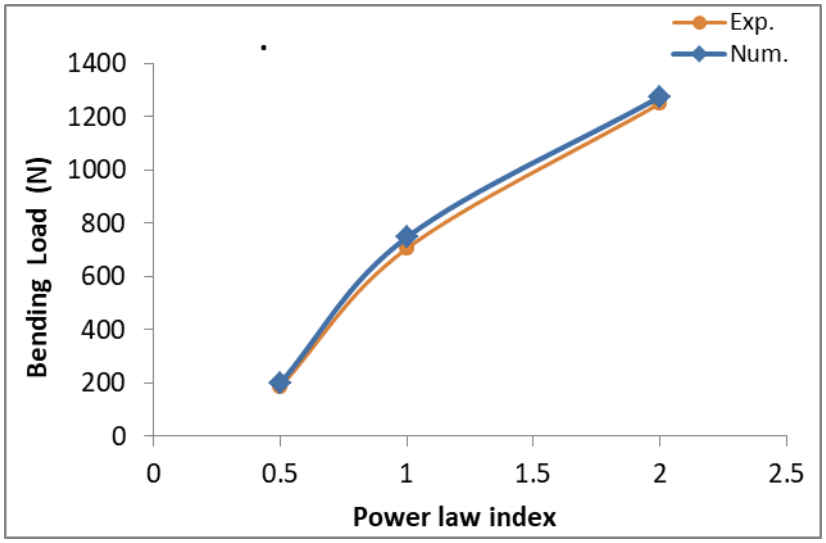

Figure (16). The results of bending load (N) with 1.5 % Al_2O_3 nanoparticles.

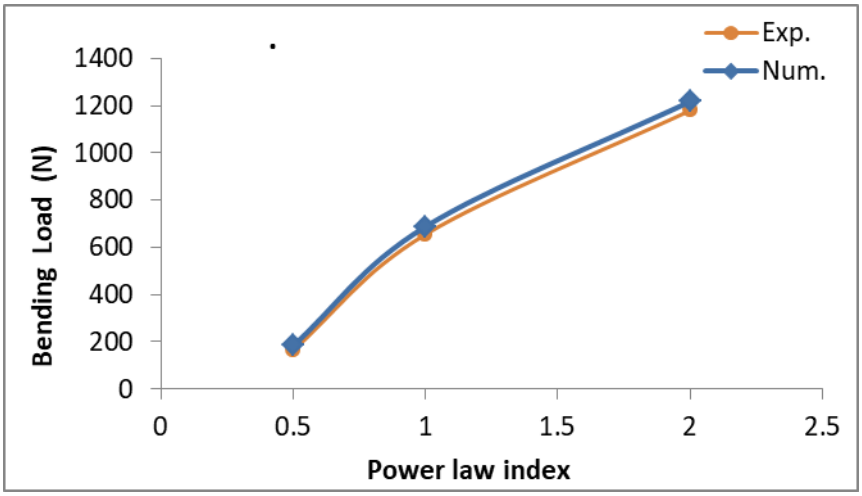

Figure (17). The results of bending load (N) with 1.5 % TiO_2 nanoparticles.

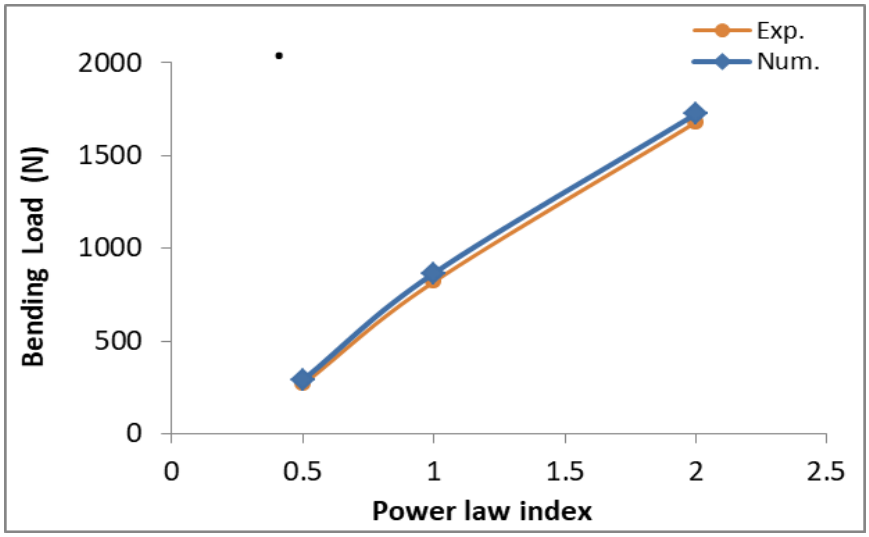

Figure (18). The results of bending load (N) with 1.5 % Al_2O_3- 3% TiO_2 nanoparticles.

Table (1). The results of bending Load (N) (Al_2O_3 nano type).

V_f %	Power-law index	Exp.	Num.	Discrepancy %
0.5	0.5	210	225	6.67
	1	798	840	5.00
	2	1465	1525	3.93
1	0.5	238	250	4.80
	1	810	845	4.14
	2	1570	1630	3.68
1.5	0.5	266	290	8.28
	1	820	866	5.31
	2	1580	1725	8.41
5	0.5	172	190	6.67
	1	733	762	5.00
	2	1300	1365	3.93

Table (2). The results of bending Load (N) (TiO_2 nano type).

V_f %	Power-law index	Exp.	Num.	Discrepancy %
0.5	0.5	218	228	4.38
	1	812	855	5.02
	2	1474	1536	4.03
1	0.5	249	258	3.48
	1	824	856	3.73
	2	1582	1645	3.83
1.5	0.5	273	289	5.54
	1	832	875	4.91
	2	1592	1747	8.87
5	0.5	188	206	4.38
	1	745	787	5.02
	2	1365	1410	4.03

Table (3). The results of bending Load (N) (Al_2O_3/ TiO_2 nano type).

V_f %	Power-law index	Exp.	Num.	Discrepancy %
1.5/1	0.5	225	249	9.64
	1	830	867	4.27
	2	1492	1567	4.79
1.5/1.5	0.5	255	278	8.27
	1	845	890	5.06
	2	1597	1675	4.66
1.5/3	0.5	298	318	6.29
	1	889	925	3.89
	2	1650	1710	3.51
1.5/5	0.5	192	211	9.64
	1	820	842	4.27
	2	1380	1417	4.79

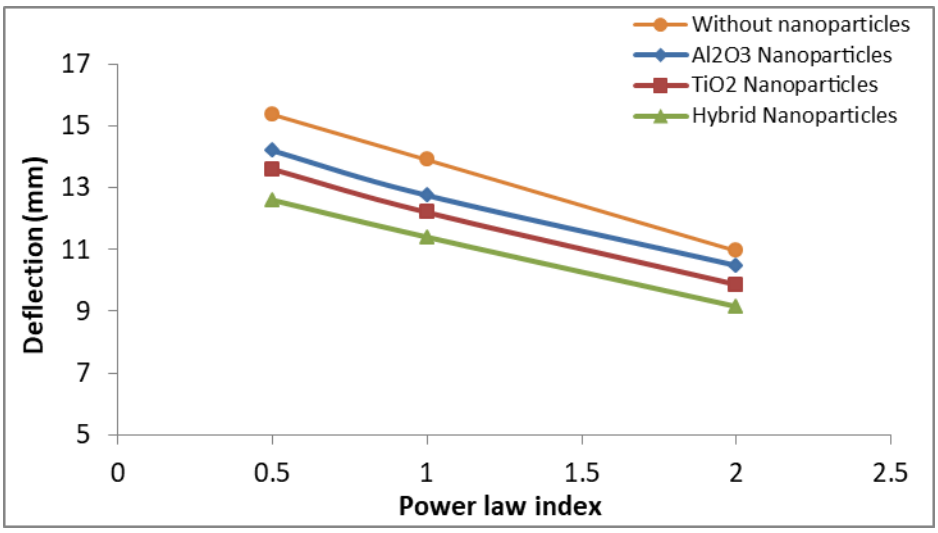

Figure (19). The experimental maximum deflection load (mm).

Table (4). The results of mid-span deflection with nanoparticles at (*n* =1).

V_f %	Nano type	Deflection(mm)
0.5	Al_2O_3	12.17
0.5	TiO_2	10.5
1.5/1	Hybrid	9.6
1	Al_2O_3	14.8
1	TiO_2	13.2
1.5/1.5	Hybrid	10.35
1.5	Al_2O_3	15.5
1.5	TiO_2	14.2
1.5/3	Hybrid	11.4
5	Al_2O_3	11.1
5	TiO_2	10.1
1.5/5	Hybrid	9.2

The deflection parameter was defined using the following dimensionless relation [35].

$$\overline{w} = \frac{100E_m bh^3}{Fl^3}.w \qquad (16)$$

Here, $\overline{(w)}$ represents the nondimensional deflection indicator, and (w) is the maximum mid-span beam deflection.

Figure (20) depicts the 3D surface created by the MATLAB environment as a function of V_f% and beam thickness of a simply-supported FG beam. According to the findings, the deflection parameter rises with V_f and beam thickness. A higher volume fraction exponent results in better variation. In this case, the beam exhibits a much higher degree of workability.

.

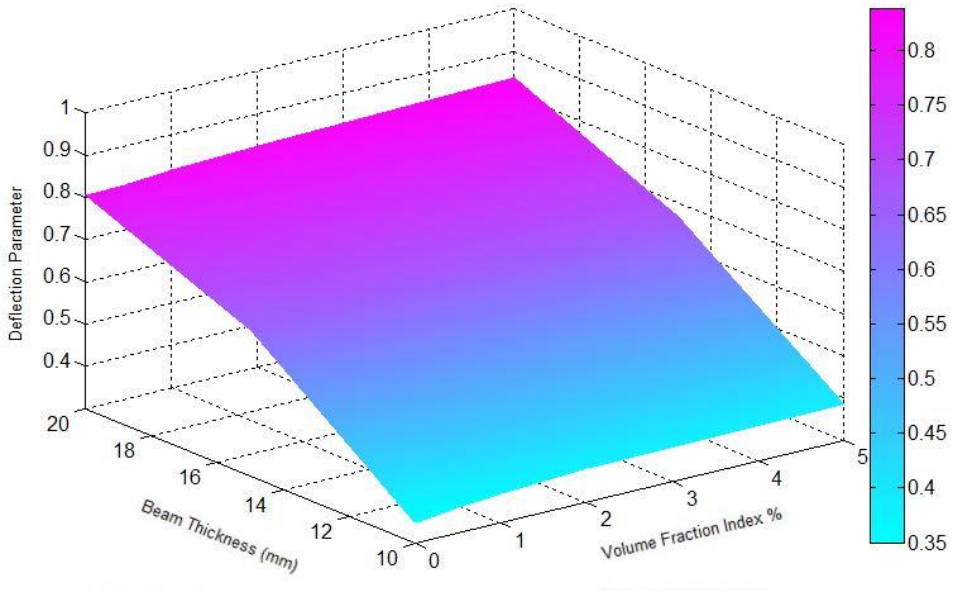

Figure (20). Surface plot of a simply supported beam with hybrid nanoparticles in 3D.

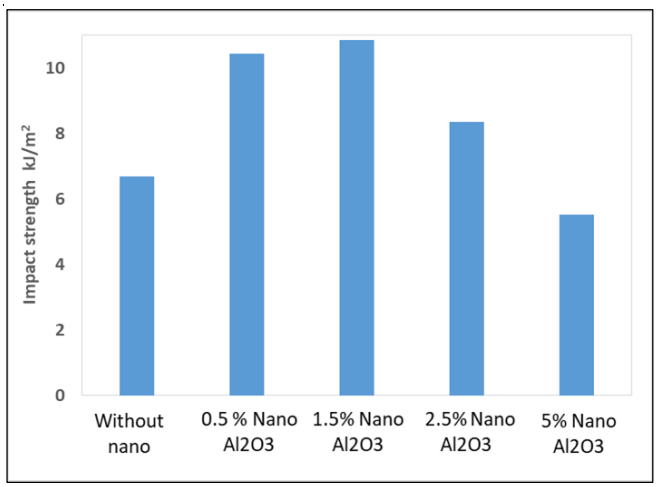

Figure (21). Impact strength of alumina NanoBeam.

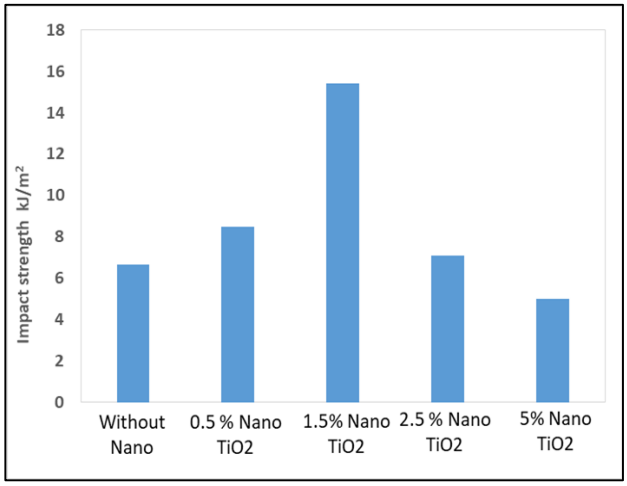

Figure (22). Impact strength of TiO_2 NanoBeam.

The highest impact strength was reported with alumina nanoparticle beams at 1.5% V_f (Figure 21), which increased by 66.7% compared to free-nano beams. When a modest amount of nano TiO_2 was added, the energy of the impact increased. However, there was a decrease in impact energy at high concentrations. As shown in Figure (22), the ultimate impact strength was obtained when particles were present (1.5% V_f), which increased by 146.15% compared to the free nano samples. The brittle nature of particles causes a decrease in the impact strength of the material. For samples of hybrid nanoparticles, the percentage of 1.0 % V_f of Al_2O_3 is fixed while changing the percentage of TiO_2 from 1.5- 5% V_f. As illustrated in Figure (23), the best impact resistance was found at 1.5 % V_f of Al_2O_3 and 3% TiO_2, where the impact resistance reached 21.75 KJ/m^2. Table (5) shows the results of the hardness and tear resistance at (n =1) at various volume fractions. From the results, one can be seen that there is a significant change in samples reinforced by hybrid nanoparticles.

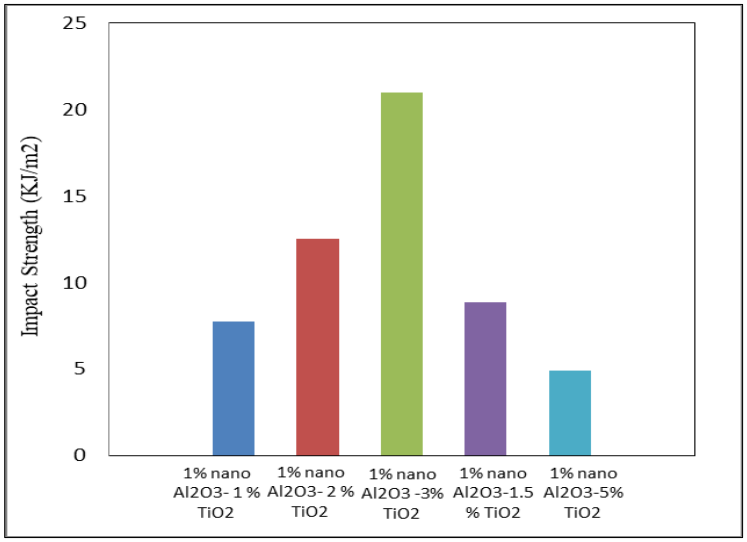

Figure (23). Impact strength of hybrid NanoBeam.

Table (5). The results of hardness and tear resistance at (n =1).

V_f %	Nano type	Hardness (IRHD)	Tear resistance (KN/m)
0.5	Al_2O_3	67	18.28
0.5	TiO_2	81	29.3
1.5/1	Hybrid	113	35.6
1	Al_2O_3	75	22.36
1	TiO_2	95	35.3
1.5/1.5	Hybrid	133	48.30
1.5	Al_2O_3	83	28.56
1.5	TiO_2	105	34.6
1.5/3	Hybrid	145	55.56
5	Al_2O_3	65	18.00
5	TiO_2	80	32.95
1.5/5	Hybrid	127	50.8

6. Conclusions

Depending on the rate at which it is loaded, a viscoelastic material has a reversible response (that is, it can return to its starting condition). This process is commonly seen in polymeric materials. The amount of applied loading also affects viscoelasticity, but the material reaction is abrupt and is characterized by persistent deformation. The flexural strength and stiffness of FGVE beams are investigated in this work. The contribution combines numerical design and experimental analysis of the nanocomposite structure. Experimental results showed that nanoparticles of (TiO_2/Al_2O_3) positively affected bending loads. At a power-law index (n = 0.5), the increase will be 17 % for samples reinforced by mixed nanoparticles (1.5% V_f of Al_2O_3 and 3% TiO_2), while at the same gradient index with only (V_f 1% Al_2O_3) nanoparticles, the increase will be 4.85%. However, samples strengthened with only (3% TiO_2) nanoparticles will show a 6.25 percent improvement. In both experimental and ANSYS analyses, a fair convergence is noticed, where the maximum error percentage is just 10% in bending and 9% in deflection measurement, which suggests that a 3D printing approach can make excellent FGVE samples. More numerical and experimental methodologies are required for designing and optimizing graded beams. For the future work and to identify the performance of FGVE beams for static and dynamic properties in detail, it is suggested to repeat the same work by fixing the percentage of TiO_2 nanoparticles while Al_2O_3 V_f nanoparticles are changed.

Acknowledgement: The Laboratory department in the State Company for Rubber and Tires Industries – Iraq and the University of Technology- Mechanical Engineering Department is helping fund some of this study's experimental work.

Conflict of Interest: The authors declare that there are no conflicts of interest associated with this research project. We have no financial or personal relationships that could potentially bias our work or influence the interpretation of the results.

References

[1] M. K. Kuzman, N. Ayrilmis, M. Sernek, and M. Kariz, “Effect of selected printing settings on viscoelastic behaviour of 3D printed polymers with and without wood,” Materials Research Express, vol. 6, no. 10. IOP Publishing, p. 105362, Sep. 13, 2019. doi: 10.1088/2053-1591/ab411c.

[2] E. K. Njim, S. H. Bakhy, and M. Al-Waily, “Free vibration analysis of imperfect functionally graded sandwich plates: analytical and experimental investigation,” *Archives of Materials Science and Engineering*, vol. 111, no. 2, pp. 49–65, 2021. doi: 10.5604/01.3001.0015.5805.

[3] S., E., Sadiq, M., J., Jweeg, and S., H., Bakhy, "Strength analysis of aircraft sandwich structure with a honeycomb core: Theoretical and Experimental Approaches," *Engineering and Technology Journal*, vol 39, no. 1, pp. 153-166, 2021.

[4] D. Bonthu, H. S. Bharath, S. Gururaja, P. Prabhakar, and M. Doddamani, "3D printing of syntactic foam cored sandwich composite," *Composites Part C: Open Access*, vol. 3, p. 100068, 2020. doi: 10.1016/j.jcomc.2020.100068.

[5] E.K. Njim, S.H. Bakhy, M. Al-Waily, "Experimental and numerical flexural analysis of porous functionally graded beams reinforced by (Al/Al_2O_3) nanoparticles, *International Journal of Nanoelectronics and Materials*, vol 15, no. 2, pp. 91-106, 2022.

[6] A. Le, S. Nimbalkar, N. Zobeiry, and S. Malek, "An efficient multi-scale approach for viscoelastic analysis of woven composites under bending," *Composite Structures*, vol. 292, p. 115698, 2022. doi: 10.1016/j.compstruct.2022.115698

[7] Y. Long, O. Rique, J. M. Fernandez, A. C. Bergan, J. E. Salazar, and W. Yu, "Simulation of the column bending test using an anisotropic viscoelastic shell model," *Composite Structures*, vol. 288, p. 115376, 2022. doi: 10.1016/j.compstruct.2022.115376.

[8] A. J. Ariza Gomez, M. Caire, L. C. A. R. Torres, and M. A. Vaz, "Bend stiffener linear viscoelastic thermo-mechanical analysis. Part I — Experimental characterization and mathematical formulation," *Marine Structures*, vol. 77. Elsevier BV, p. 102946, May 2021. doi: 10.1016/j.marstruc.2021.102946.

[9] Y. Gao, F. Yu, and P. Wu, "Exact analytical solutions for bending creep behavior of viscoelastic laminated arches with interlayers," *Thin-Walled Structures*, vol. 174, p. 109128, 2022. doi: 10.1016/j.tws.2022.109128.

[10] S. Chen, B. Tai, and J. Wang, "An experimental study of 3D printing based viscoelastic bimaterial subjected to low-velocity impact," *Mechanics of Materials*, vol. 176, p. 104508, 2023. doi: 10.1016/j.mechmat.2022.104508

[11] M. Anthony Xavior, D. Nishanth, N. Navin Kumar, and P. Jeyapandiarajan, "Synthesis and Testing of FGM made of ABS Plastic Material," *Materials Today: Proceedings*, vol. 22. Elsevier BV, pp. 1838–1844, 2020. doi: 10.1016/j.matpr.2020.03.018.

[12] A. Dogan, "Quasi-static and dynamic response of functionally graded viscoelastic plates," *Composite Structures*, vol. 280, p. 114883, 2022. doi: 10.1016/j.compstruct.2021.114883.

[13] N. K. Sahu, D. K. Biswal, S. V. Joseph, and S. C. Mohanty, "Vibration and damping analysis of doubly curved viscoelastic-FGM sandwich shell structures using FOSDT," *Structures*, vol. 26, pp. 24–38, 2020. doi: 10.1016/j.istruc.2020.04.007.

[14] A. I. Aria, T. Rabczuk, and M. I. Friswell, "A finite element model for the thermo-elastic analysis of functionally graded porous nanobeams," *European Journal of Mechanics - A/Solids*, vol. 77, p. 103767. doi: 10.1016/j.euromechsol.2019.04.002.

[15] M. Al-Waily, M.J. Jweeg, M.A. Al-Shammari, K.K. Resan, and A.M. Takhakh, "Improvement of Buckling Behavior of Composite Plates Reinforced with Hybrids Nanomaterials Additives," *Materials Science Forum*, pp. 23-41, 2021.

[16] G. Liu, S. Wu, D. Shahsavari, B. Karami, and A. Tounsi, "Dynamics of imperfect inhomogeneous nanoplate with exponentially-varying properties resting on viscoelastic foundation," *European Journal of Mechanics - A/Solids*, vol. 95, p. 104649, 2022. doi: 10.1016/j.euromechsol.2022.104649.

[17] B. R. Lokesh Yadhav, H. K. Govindaraju, M. D. Kiran, and B. Suresha, "Three-point bending and impact behaviour of carbon/epoxy composites modified with titanium dioxide nanoparticles," *Materials Today: Proceedings*, vol. 43, pp. 1755–1761, 2021. doi: 10.1016/j.matpr.2020.10.442.

[18] P. Yu, W. Leng, L. Peng, Y. Suo, and J. Guo, "The bending and vibration responses of functionally graded piezoelectric nanobeams with dynamic flexoelectric effect," *Results in Physics*, vol. 28, p. 104624, 2021. doi: 10.1016/j.rinp.2021.104624.

[19] Y. Gafour, A. Hamidi, A. Benahmed, M. Zidour, and T. Bensattalah, "Porosity-dependent free vibration analysis of FG nanobeam using non-local shear deformation and energy principle," *Advances in nano research*, vol. 8, no. 1, pp. 37–47, Jan. 2020, doi: 10.12989/ANR.2020.8.1.037.

[20] T. Hai, M. M. Al-Masoudy, S. Alsulamy, M. Hechmi El Ouni, A. Ayvazyan, and A. Kumar, "Moving load analysis on cross/angle-ply laminated composite nanoplates resting on viscoelastic foundation," *Composite Structures*, vol. 305, p. 116540, Feb. 2023. doi: 10.1016/j.compstruct.2022.116540.

[21] K. Koutoati, F. Mohri, E. M. Daya, and E. Carrera, "A finite element approach for the static and vibration analyses of functionally graded material viscoelastic sandwich beams with nonlinear material behavior," *Composite Structures*, vol. 274, p. 114315, doi: 10.1016/j.compstruct.2021.114315.
[22] S. K. Alavi, M. R. Ayatollahi, M. Petrů, and S. S. R. Koloor, "On the dynamic response of viscoelastic functionally graded porous plates under various hybrid loadings," *Ocean Engineering*, vol. 264, p. 112541, 2022. doi: 10.1016/j.oceaneng.2022.112541.
[23] T. Hai, M. M. Al-Masoudy, S. Alsulamy, M. Hechmi El Ouni, A. Ayvazyan, and A. Kumar, "Moving load analysis on cross/angle-ply laminated composite nanoplates resting on viscoelastic foundation," *Composite Structures*, vol. 305, p. 116540, 2023. doi: 10.1016/j.compstruct.2022.116540.
[24] R. Shi et al., "Tensile performance and viscoelastic properties of rubber nanocomposites filled with silica nanoparticles: A molecular dynamics simulation study," *Chemical Engineering Science*, vol. 267, p. 118318, 2023. doi: 10.1016/j.ces.2022.118318.
[25] M. Al-Shablle, M. Al-Waily, and E. K. Njim, "Analytical evaluation of the influence of adding rubber layers on free vibration of sandwich structure with presence of nano-reinforced composite skins," *Archives of Materials Science and Engineering*, vol. 116, no. 2, pp. 57–70, 2022. doi: 10.5604/01.3001.0016.1190.
[26] E. K. Njim, S. H. Bakhy, and M. Al-Waily, "Analytical and numerical free vibration analysis of porous functionally graded materials (FGPMs) sandwich plate using Rayleigh-Ritz method," *Archives of Materials Science and Engineering*, vol. 1, no. 110, pp. 27–41, 2021. doi: 10.5604/01.3001.0015.3593.
[27] E. K. Njim, S. H. Bakhy, and M. Al-Waily, "Analytical and Numerical Investigation of Free Vibration Behavior for Sandwich Plate with Functionally Graded Porous Metal Core," *Pertanika Journal of Science and Technology*, vol. 29, no. 3, 2021. doi: 10.47836/pjst.29.3.39.
[28] E.K. Njim, S.H. Bakhy, and M. Al-Waily, "Analytical and numerical flexural properties of polymeric porous functionally graded (PFGM) sandwich beams," *Journal of Achievements in Materials and Manufacturing Engineering*, vol. 110, no. 1, pp. 5–10, 2022. doi: 10.5604/01.3001.0015.7026.
[29] ASTM D638, "standard test method for tensile properties of plastics," Annual Book of ASTM Standards, *American Society of Testing and Materials*, West Conshohocken, 2014.
[30] ASTM D790 "Standard test methods for flexural properties of unreinforced and reinforced plastics and electrical insulating materials," ASTM International, West Conshohocken, Pa, United States, 2014.
[31] R. Alaa Mohammed, "Effect of Al_2O_3 Powder on Some Mechanical and Physical Properties for Unsaturated Polyester Resin Hybrid Composites Materials Reinforced by Carbon and Glass Fibers," *Engineering and Technology Journal*, vol. 34, no. 12, pp. 2371–2379, 2016. doi: 10.30684/etj.34.12a.18.
[32] E. K. Njim, S. H. Bakhy, and M. Al-Waily, "Optimisation Design of Functionally Graded Sandwich Plate with Porous Metal Core for Buckling Characterisations," *Pertanika Journal of Science and Technology*, vol. 29, no. 4, 2021. doi: 10.47836/pjst.29.4.47.
[33] P. Van Vinh and L. Q. Huy, "Finite element analysis of functionally graded sandwich plates with porosity via a new hyperbolic shear deformation theory," *Defence Technology*, vol. 18, no. 3, pp. 490–508, 2022. doi: 10.1016/j.dt.2021.03.006.
[34] M.-O. Belarbi, M. S. A. Houari, H. Hirane, A. A. Daikh, and S. P. A. Bordas, "On the finite element analysis of functionally graded sandwich curved beams via a new refined higher order shear deformation theory," *Composite Structures*, vol. 279, p. 114715, 2022. doi: 10.1016/j.compstruct.2021.114715.
[35] M. D. Do, M. T. Tran, and H. C. Truong, "Bending Analysis of Sandwich Beam with Functionally Graded Face Sheets Using Various Beam Theories by Meshfree Method," Kalpa Publications in Engineering. EasyChair. doi: 10.29007/9nvf.